Structure Development in the Phenolic Resin–Poly(styrene-ran-acrylonitrile) Copolymer Blends

BONG SUP KIM,[1] GEN-ICHI NAKAMURA,[2] TAKASHI INOUE[2]

[1] R&D Center, SK Chemicals, 600 Jungja 1-Dong, Changan-Ku, Suwon, Kyungki 440-745, Korea

[2] Department of Organic and Polymeric Materials, Tokyo Institute of Technology, 2-12-1 Ookayama, Meguro-Ku, Tokyo 152, Japan

Received 15 October 1997; accepted 3 April 1998

ABSTRACT: Single-phase mixtures of phenolic derivatives with poly(styrene-ran-acrylonitrile) copolymers (SAN) were cured in the presence of hexamethylenetetramine, and the effect of the acrylonitrile (AN) content in SAN on the phase separation and reaction kinetics during curing were investigated by light scattering, differential scanning calorimetry (DSC), and optical microscopy (OM). DSC measurements revealed that the reaction rate does not have a significant effect on the AN content in SAN but depended on the fraction of multifunctional phenols in total phenols. The time variation of the light scattering profile during cure demonstrated the characteristic feature for spinodal decomposition. OM observation revealed that a co-continuous two-phase structure appeared after a certain time lag and coarsened to a spherical domain structure consisting of phenolic-rich particles dispersed in the SAN-rich matrix. The periodic distance, Λ_m in the phase-separated structure changed with curing time, as follows. The higher the miscibility between phenolic resin and SAN, the higher the fraction of multifunctional phenols in total phenols, the higher the SAN composition, and the lower the cure temperature, the shorter the Λ_m was. © 1998 John Wiley & Sons, Inc. J Appl Polym Sci 70: 757–764, 1998

Key words: phenolic; poly(styrene-ran-acrylonitrile); conversion; gelation; phase separation; AN content

INTRODUCTION

Phenolic resin is one of the most important thermosetting resins. It has many desirable properties, such as good heat resistance, excellent chemical resistance, and good dimensional stability. Consequently, it is widely used for many important applications, such as structural adhesives, insulating material for electric and electronic components, reinforced plastics, and matrix resins for advanced composite materials.[1–3] However, it is inherently brittle due to the higher crosslinking density and, consequently, has limited use in applications requiring high impact strength. This problem can be moderated by incorporating the elastomeric and/or thermoplastic polymers into phenolics. So far, various attempts to enhance the impact strength of thermosetting resins by modification with elastomeric and/or thermoplastic polymers have been reported in the literature. However, most studies have focused on epoxy resins,[4–10] and very limited information has been reported on the structure development and impact strength enhancement for phenolic resins. ICI Fiberite[11] has developed a thermoplastic-toughened phenolic matrix for use in fiber

Correspondence to: B. S. Kim.

Journal of Applied Polymer Science, Vol. 70, 757–764 (1998)
 CCC 0021-8995/98/040757-08

composites. They designed and developed a thermoplastic with various thermoplastic backbones, molecular weights, and natures of end group functionalities. Shu and Konii[12] have developed the modified phenolic resin in which some portion of phenolic hydroxyl groups was reacted with alkyl titanate and the modified phenolic resin was cured by hexamethylenetetramine. Culbertson et al.[13] have studied the modification of phenolic resin, which was cured by phenylene–bisoxazoline. Matsumoto et al.[14] have reported that the modification of phenolic resin by *p*-hydroxyphenylmaleimide–acrylic ester copolymer improves both flexural strength and heat resistance.

In our previous article,[15,16] we described the effects of the crosslinking density of phenolic resins and medium viscosity of poly(methyl methacrylate-*co*-ethyl acrylate)[P(MMA-*co*-EA)] copolymers on the reaction kinetics and phase separation in the phenolic resin–P(MMA-*co*-EA) mixture. And we found that a graft reaction could be taken place between PMMA and phenolic resins. This result in a grafted phenolic resin–PMMA interpenetrating polymer network having an excellent chemical resistance.

In this article, we employed the mixtures of phenolic derivatives (phenolics) with poly(styrene-ran-acrylonitrile) copolymers (SAN) with various AN contents and studied the reaction kinetics by differential scanning calorimetry (DSC), the phase separation process by light scattering, and morphological development by optical microscopy to investigate the effect of AN content of SAN on the miscibility and structure development in phenolics–SAN mixtures during curing of phenolics.

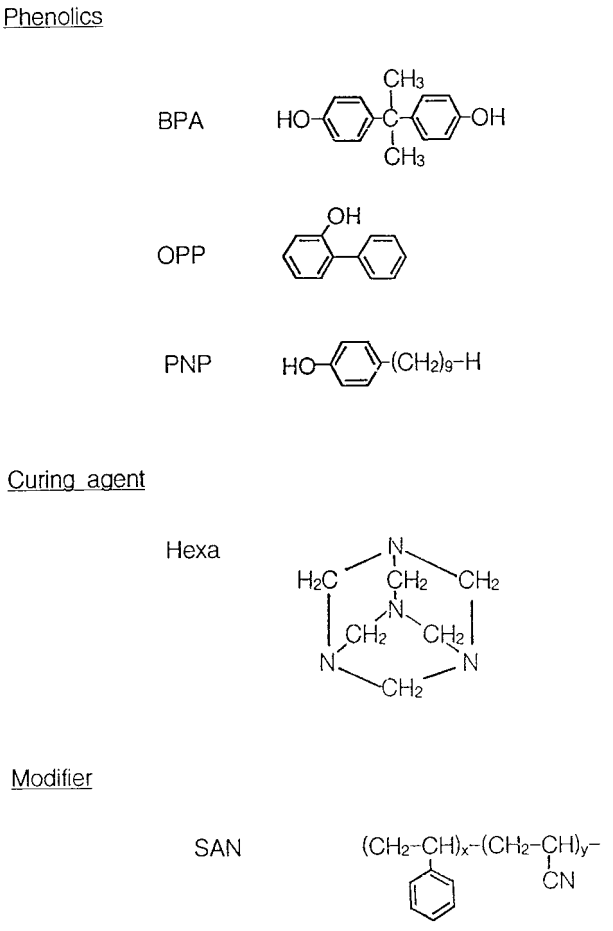

Scheme 1

EXPERIMENTAL

A bisphenol A (BPA; $M_w = 228\ gmol^{-1}$) was supplied by Wako Chemical Co. A *p*-nonyl phenol (PNP; $M_w = 220\ gmol^{-1}$) and *o*-phenyl phenol (OPP; $M_w = 170\ gmol^{-1}$) were supplied by Tokyo Kasei Chemical Co. The curing agent was hexamethylenetetramine (Hexa). A poly(styrene-ran-acrylonitrile) copolymer (SAN) with various AN contents, 10 (SAN-10; $M_w = 300\ K\ gmol^{-1}$), 25 (SAN-25; $M_w = 150\ K\ gmol^{-1}$), and 40% (SAN-40; $M_w = 80\ K\ gmol^{-1}$) were supplied by Mitsubishi Monsanto Co. Polystyrene (PS) (SAN-0; $M_w = 180\ K\ gmol^{-1}$) was supplied by Tenki Chemical Inc. The structure formulae of materials employed are shown in Scheme 1.

A poly(*o*-phenyl phenol) (POPP) was prepared by bulk polymerization of *o*-phenyl phenol (OPP) with Hexa. At first, OPP (35 mmol) and Hexa (35 mmol) was added to a glass tube, and the mixture was preheated to 160°C. After thorough mixing, the mixture was sealed and polymerized at 180°C for 5 h, and further polymerization was performed at 220°C for 2 h. A molecular weight of POPP obtained was measured by gel permeation chromatography (GPC) and was 1680 $gmol^{-1}$.

The desired amounts of POPP and SANs with various AN contents, 0, 10, 25, and 40%, were dissolved in dichloromethane at 10 wt % of total polymer. The solutions were cast onto a cover glass (for microscopy). The cast films were further dried under a vacuum of 10^{-4} mm Hg for 12 h. The mixture specimens thus obtained were transparent at all over the compositions, and no phase-separated morphology was detected under the optical microscopic observation. And the specimens

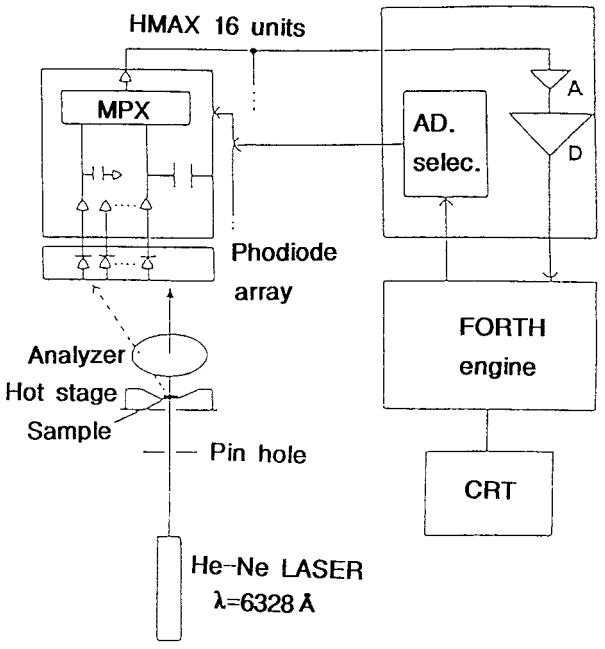

Figure 1 Light scattering apparatus.

were inserted in a heating stage for the cloud point measurements. Upon annealing the film at a certain temperature, we observed the phase-separated morphology under optical microscope. Based on this observation, the phase diagrams of the POPP/SANs mixtures were obtained.

We also prepared in the same way as the solution-cast specimens of the (BPA + OPP)/Hexa/SANs and (BPA + PNP)/Hexa/SANs mixtures with various AN contents. These mixtures also show homogeneous single phase, as prepared. The film specimens cast onto a cover glass were inserted into the heating stage of the light scattering apparatus, whose schematic diagram is given in Figure 1, and allowed to experience an isothermal heating. Radiation from a He–Ne gas laser (wavelength 632.8 nm) was applied vertically to the film. The intensity of scattered light from the film was measured under an optical alignment with parallel polarization (V_v). The angular distribution of scattered light intensity was detected by a one-dimensional photometer with a 46 photodiode array (HASC Co. Ltd). The scattering profiles in a time of 1/30 s were recorded at the appropriate intervals during the isothermal annealing (curing of BPA, PNP, and OPP with Hexa and consequent phase separation) and were stored in a Forth Engine computer for the analysis. The scattering angle, θ, within the specimen is related to the observed scattering angle, θobs, by

$$n \sin \theta = \sin \theta\text{obs}$$

where n is the refractive index of the specimen. The intensity of scattered light was corrected by multiplying Cn, as follows:

$$Cn = n^2 \cos \theta/(1 - n^2 \sin \theta)^{1/2}$$

A light scattering pattern was also observed by using a photographic technique.[17]

The kinetics of curing reaction was examined by DSC (Du Pont, model 910). The heat of reaction for the uncured mixture was determined from the DSC run at a heating rate of 10°C min^{-1} over the temperature range of 100–350°C. And the heat of reaction occurring during the isothermal curing was obtained by measuring with the same procedure, as above, for the heat of reaction for the already cured mixture and substracting it from that of the cured one. Therefore, the conversion (degree of reaction) of the cured mixture up to a given reaction time were estimated by comparing the areas under the exotherm peaks and is given by the following equation:

$$\text{Conversion } (\%) = (1 - A_t/A_0) \times 100$$

where A_0 is the area of exotherm peak of uncured material, and A_t is that of the cured one.

A theoritical conversion at the gelation point was calculated using the Flory–Stockmayer gelation theory.[18–20]

RESULTS AND DISCUSSION

Phase Diagrams of POPP–SANs Mixtures

Figure 2 shows phase diagrams of POPP–SANs mixtures with various AN contents in SAN. The POPP–PSANs mixtures have a lower critical solution temperature LCST-type phase behavior as shown in Figure 2. The LCST of a POPP blend with SAN-25 is lower than that with SAN-0, SAN-10, and SAN-40. It may be caused by the miscibility enhancement due to the strong polymer–polymer interaction in SAN-25. The T_gs of POPP–SANs mixtures, estimated by the Fox equation using the T_g data of neat POPP and SAN, which were measured by DSC, are also shown in Figure 2.

Upon our current understanding of polymer–polymer miscibility, the LCST is expected to decrease as the molecular weight of a thermosetting

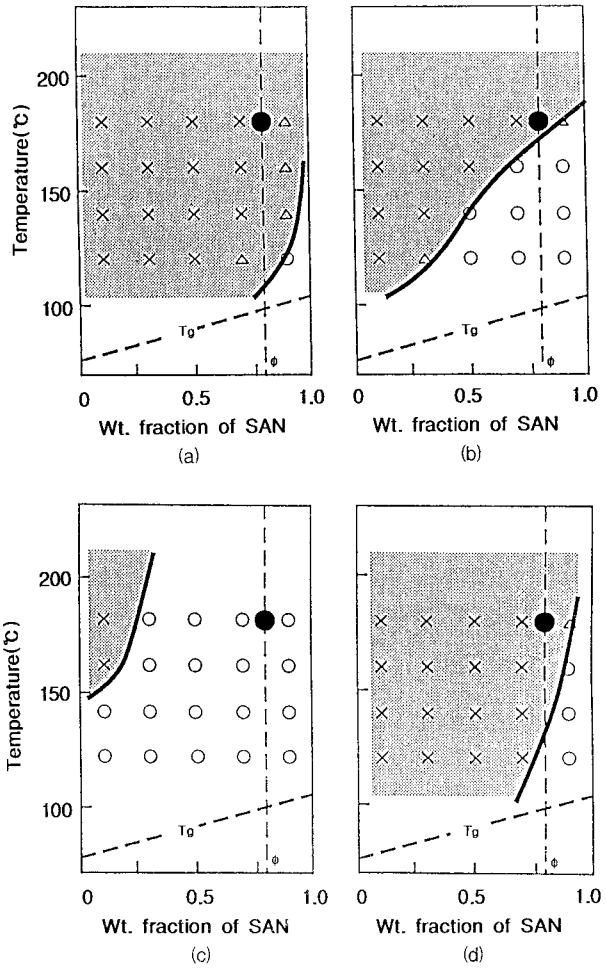

Figure 2 Phase diagrams of the POPP–SAN with various AN content mixtures: (a) 0; (b) 10; (c) 25; (d) 40%.

resin, that is, POPP in our case, increase with curing, and then the two-phase region would preveil in the phase diagram with curing of POPP. The T_g of mixture would be elevated when the molecular weight of POPP increases. These situations are demonstrated schematically in Figure 3. Figure 3 implies that the mixture with composition ϕ is initially at a single-phase at an isothermal curing temperature, T_{cure}; however, the system will be thrust into a two-phase region as the curing reaction proceeds. Hence, the spinodal decomposition is expected to take place in the curing process.

Structure Developments of (BPA + OPP)–Hexa–SANs and (BPA + PNP)–Hexa–SANs Mixtures by Light Scattering

As-cast film of a (BPA + OPP)–Hexa–SAN-0 (3.2 + 12.8)/4/80 wt % mixture was a homogeneously mixed single phase system and no appreciable light scattering was detected from the mixture in the very early stages of an isothermal curing at 180°C. After some induction period, a ring pattern of light scattering appeared. The ring pattern implies that with curing, a regularly phase-separated structure were developed in the mixture. The ring pattern became brighter, and its diameter decreased with curing time. A typical example of the change in the light scattering profile is presented in Figure 4. The characteristic changes on scattering profile shown in Figure 4 are the hallmarks of spinodal decomposition.

In order to discuss a domain spacing of phase-separated structure, we estimate the periodic distance, Λ_m, in the phase-separated structure as a Bragg spacing from the peak angle, θ_m, of the scattering profile in Figure 4. Λ_m is given by

$$\Lambda_m = 2\pi/q,\ q = (4\pi/\lambda)\sin(\theta_m/2)$$

Therefore,

$$\Lambda_m = \lambda\ [2n\ \sin(\theta_m/2)]^{-1}$$

where q is the scattering vector, λ is the wavelength of the light in the medium, and n is refractive index.

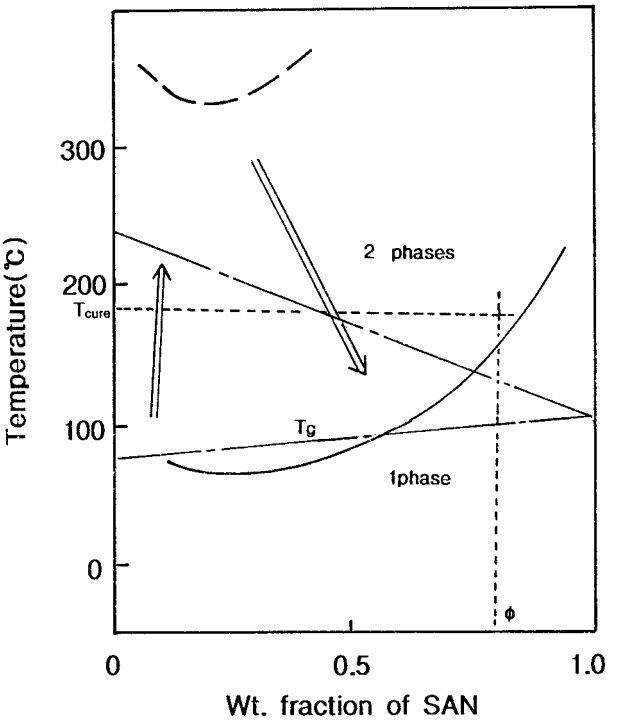

Figure 3 Schematic representation of the variation of phase diagram and T_g with curing.

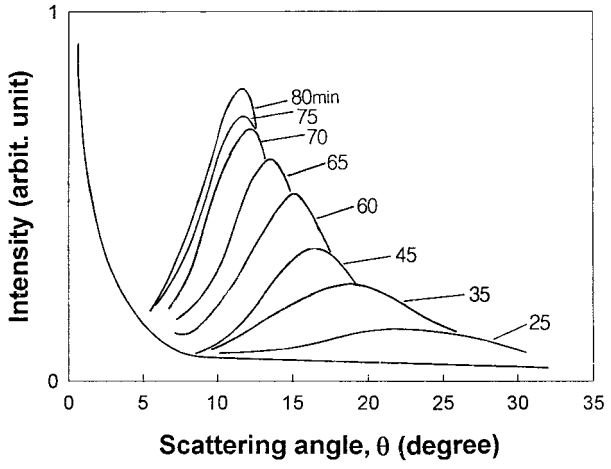

Figure 4 Light scattering profile of (BPA + OPP)–Hexa–SAN-10 = (1.6 + 14.4)/4/80 wt %) mixture during cure at 180°C.

The time variation of Λ_m in (BPA + PNP)–Hexa–SAN with various AN contents (1.6 + 14.4)/4/80 wt % mixtures during cure at 180°C is plotted in Figure 5. The Λ_m increases with cure time, indicating a structure coarsening, and then levels off due to the network formation in phenolic-rich phase. For the SAN-0 system, the Λ_m is higher than that of SAN-10 and SAN-25 system. On the other hand, Figure 6 shows the change of the Λ_m by AN content in SAN and cure temperature in (BPA + PNP)–Hexa–SANs with various AN contents (1.6 + 14.4)/4/80 wt % mixtures. The larger the AN content in SAN, the shorter the Λ_m in the phase-separated structure. Especially, the phenolic–SAN-25 system has the shortest the Λ_m due to the strong polymer–

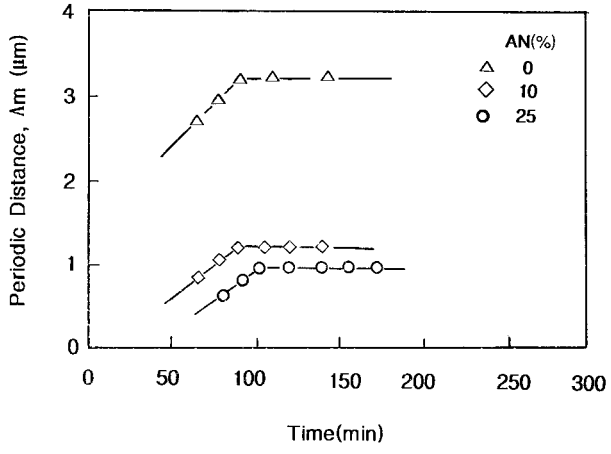

Figure 5 Time variation of periodic distance of (BPA + PNP)–Hexa–SAN with various AN contents = (1.6 + 14.4)/4/80 wt %) mixture during cure at 180°C.

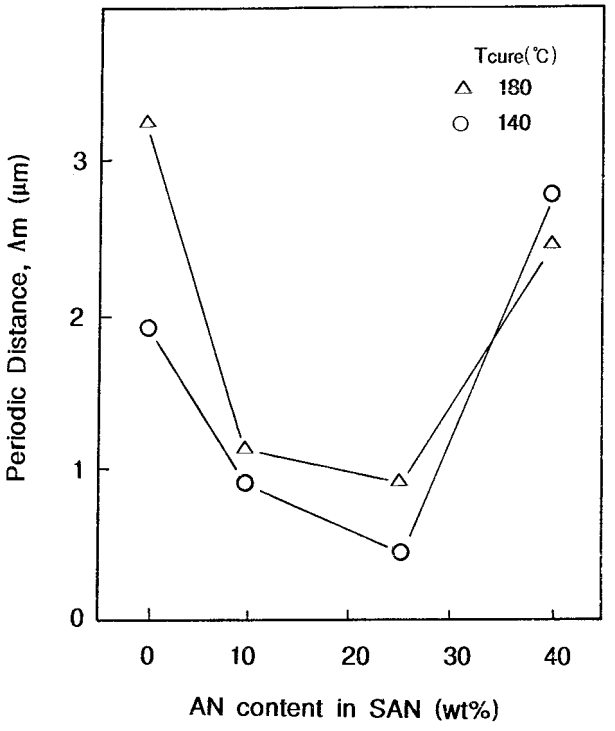

Figure 6 Change in periodic distance of (BPA + PNP)–Hexa–SAN with various AN contents = (1.6 + 14.4)/4/80 wt %) mixture during cure at various cure temperature.

polymer interaction in SAN copolymer. Also, the lower the cure temperature, the shorter the Λ_m. Figure 7 shows the change of the Λ_m by AN content in SAN and cure temperature in (BPA + OPP)–Hexa–SANs with various AN contents (3.2 + 12.8)/4/80 wt % mixtures. As shown in Figure 7, the larger the AN content in SAN and the lower the cure temperature, the shorter the Λ_m in phase-separated structure. Especially, the phenolic–SAN-25 system has the shortest the Λ_m due to the strong polymer–polymer interaction in SAN copolymer. On the other hands, the effect of SANs–phenolic composition on the Λ_m in SANs–(BPA + OPP)–Hexa mixtures is shown in Tables I and II. As can be seen in the tables, the periodic distance, Λ_m, in the phase-separated structure changed with curing time. The higher the miscibility between phenolic resin and SAN, the higher the fraction of multifunctional phenols in total phenols, the higher the SAN composition, and the lower the cure temperature, the shorter the periodic distance.

Cure Kinetics

Figure 8 shows the time–conversion curves of (BPA + PNP)–Hexa–SAN-10 = [(16 + 0)/4/80 wt % and

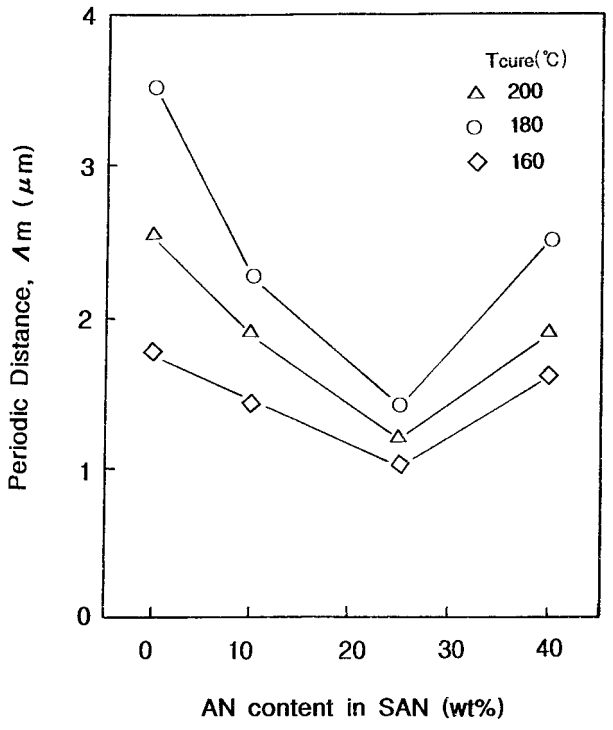

Figure 7 Change in periodic distance of (BPA + OPP)–Hexa–SAN with various AN contents = (3.2 + 12.8)/4/80 wt %) mixture during cure at various cure temperature.

(BPA + PNP)–Hexa–SAN-10 = (1.6 + 14.4)/4/80 wt %) mixtures during cure at 180°C. As expected, the reaction rate of (BPA + PNP)–Hexa–SAN-10 = [(16 + 0)/4/80 wt % system was faster than that of (BPA + PNP)–Hexa–SAN-10 = (1.6 + 14.4)/4/80 wt %) mixtures. In order to investigate the effect of fraction of multifunctional phenols in total phenols, we employ a various derivatives mixtures of BPA + PNP, BPA + OPP, and BPA. The reaction rate of the BPA–Hexa–SAN mixture is faster than that of (BPA + OPP) and (BPA + PNP) mixture. It may be

Table I The Effect of SANs–Phenolic Composition on the Λ_m in SANs–(BPA + OPP = 2/8)–Hexa Blends Cured at 180°C.

AN Content (%)	Periodic Distance [Λ_m (μm)] SAN–Phenolic Composition (wt %)		
	75/25	70/30	65/35
0	4.03	4.26	4.54
10	3.02	3.15	3.02
25	1.92	2.02	1.59
40	2.02	2.69	2.27

Table II The Effect of BPA–OPP Ratio on the Λ_m in SANs–Phenolic = 65/35 Blends Cured at 180°C

AN Content (%)	Periodic Distance (Λ_m (μm) BPA–OPP Ratio	
	1/9	2/8
0	4.54	4.54
10	4.27	3.02
25	1.35	1.59
40	2.14	2.27

caused by a higher reactivity due to the higher fraction of multifunctional phenols in total phenols. According to the Flory–Stockmayer gelation theory,[18,19] the conversion at gelation decreases with increasing a functionality of the reactants. For a system containing a mixture of OPP, PNP, and BPA with a functionalities of 2, 2, and 4, respectively, and Hexa, in which Hexa can only react with phenolic monomer, the critical extent of reaction at the gel point (P_c) is given by the following equation.

$$P_c^2 = r[(f_{\text{phenol}} - 1)(g_{\text{Hexa}} - 1)]^{-1}$$

where r is the molar ratio of reacting groups in phenolic resins to Hexa, and f_{phenol} and g_{Hexa} are the functionalities of the phenolic resin and Hexa,

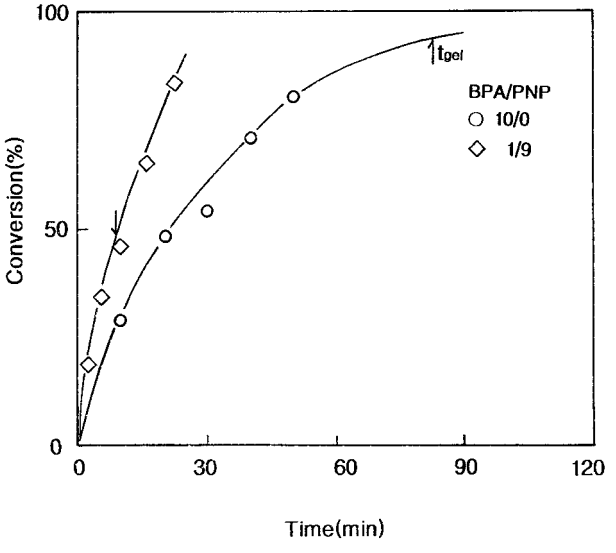

Figure 8 Time–conversion curves of (BPA + PNP)–Hexa–SAN-10 = (16 + 0)/4/80 wt %) and (BPA + PNP)–Hexa–SAN = (1.6 + 14.4)/4/80 wt %) mixtures during cure at 180°C.

respectively. Let us calculate the critical extent of reaction at the gel point (P_c) as in the following cases. For (BPA + PNP)–Hexa = (1.0 + 0)/1,

$$P_c^2 = \frac{1}{(f_{\text{phenol}} - 1)(g_{\text{Hexa}} - 1)}$$

where $P_c = 0.577$ and

$$X_n = \frac{f + 2}{(1 - 2P)f + 2} = 4.33$$

For (BPA + PNP)–Hexa = (0.2 + 0.8)/1,

$$\frac{r\,P_c^2\,\rho}{1 - r\,P_c^2\,(1 - \rho} = \frac{1}{(f_{\text{phenol}} - 1)(g_{\text{Hexa}} - 1)}$$

where $P_c = 0.845$ and

$$X_n = \frac{f(1 - \rho + 1/r) + 2\rho}{f(1 - \rho + 1/r - 2P) + 2\rho} = 9.05$$

For (BPA + PNP)–Hexa = (0.1 + 0.9)/1,

$$\frac{r\,P_c^2\,\rho}{1 - r\,P_c^2\,(1 - \rho)} = \frac{1}{(f_{\text{phenol}} - 1)(g_{\text{Hexa}} - 1)}$$

where $P_c = 0.913$ and

$$X_n = \frac{f(1 - \rho + 1/r) + 2\rho}{f(1 - \rho + 1/r - 2P) + 2\rho} = 15.72$$

In these cases, ρ and $1 - \rho$ are the fraction of BPA and PNP, respectively, and X_n is the degree of polymerization at gelation. Hence, the theoretical conversion at gelation for (BPA + PNP)–Hexa = (1 + 0)/1 and (BPA + PNP)–Hexa = (0.2 + 0.8)/1 and (BPA + PNP)–Hexa = (0.1 + 0.9)/1 mixtures are 0.577, 0.845, and 0.913, respectively. The X_n for (BPA + PNP)–Hexa = (1 + 0)/1 and (BPA + PNP)–Hexa = (0.2 + 0.8)/1 and (BPA + PNP)–Hexa = (0.1 + 0.9)/1 mixtures are 4.33, 9.05, and 15.72, respectively. This means that the higher the fraction of multifunctional phenols, BPA, in total phenols, the smaller the value of P_c and the higher the value of X_n.

Morphology Observation by Optical Microscopy

Under the microscope, the as-cast transparent specimen of (BPA + OPP)–Hexa–SAN mixtures remained the same for some period of time after a temperature jump from room temperature to the curing temperature. After a certain time lag, a two-phase structure with low contrast appeared, and the contrast became higher with further curing. Figure 9 shows optical micrographs of (BPA + OPP)–Hexa–SAN-0 and SAN-25 = (1.6 + 14.4)/4/80 wt %) mixture cured at 180°C. The micrographs clearly show the uniform interdomain spacing and uniform domain size, and then the phase-separated structure became a spherical at the late stage of curing. The regularly phase-separated structure is quite similar to the spinodal decomposition pattern. The periodic distance in phase-separated structure of (BPA + OPP)–Hexa–SAN-25 = (1.6 + 14.4)/4/80 wt %) mixture is smaller than that of the (BPA + OPP)–Hexa–SAN-0 = (1.6 + 14.4)/4/80 wt %) mixture. It may be caused by the strong polymer–polymer interaction in SAN. That is, the phase separation is suppressed by the faster gelation in phenolic-rich phase so that the phase-separated structure can be fixed by the network formation in phenolic-rich phase at the early stage of spinodal decomposition. These results in a two-phase structure became spherical in shape at the late stage of curing. This is consistent with the light scattering profiles presented Figure 4. This may be caused that it could be suppressed by the formation of phenolic network before phase separation occurs.

CONCLUSIONS

Single-phase mixtures of phenolic derivatives with poly(styrene-ran-acrylonitrile) copolymer (SAN) having various AN contents of 0, 10, 25, and 40% were cured in the presence of hexamethylenetetramine, and the phase separation and cure kinetics processes during cure were investigated by light scattering, DSC, and optical microscopy (OM). DSC measurements revealed that the reaction rate has no significant effect on the AN content in SAN but depended on the fraction of multifunctional phenols in total phenols. The time variation of light scattering profile during cure demonstrated the characteristic feature for spinodal decomposition. OM observation revealed that co-continuous two-phase structure appeared after a certain time lag and coarsened to a spherical domain structure consisting of phenolic-rich particles dispersed in the SAN-rich matrix. The periodic distance, Λ_m, in the phase-separated structure changed with curing time. The higher the miscibility between phenolic resin and SAN, the higher the fraction of multifunctional phe-

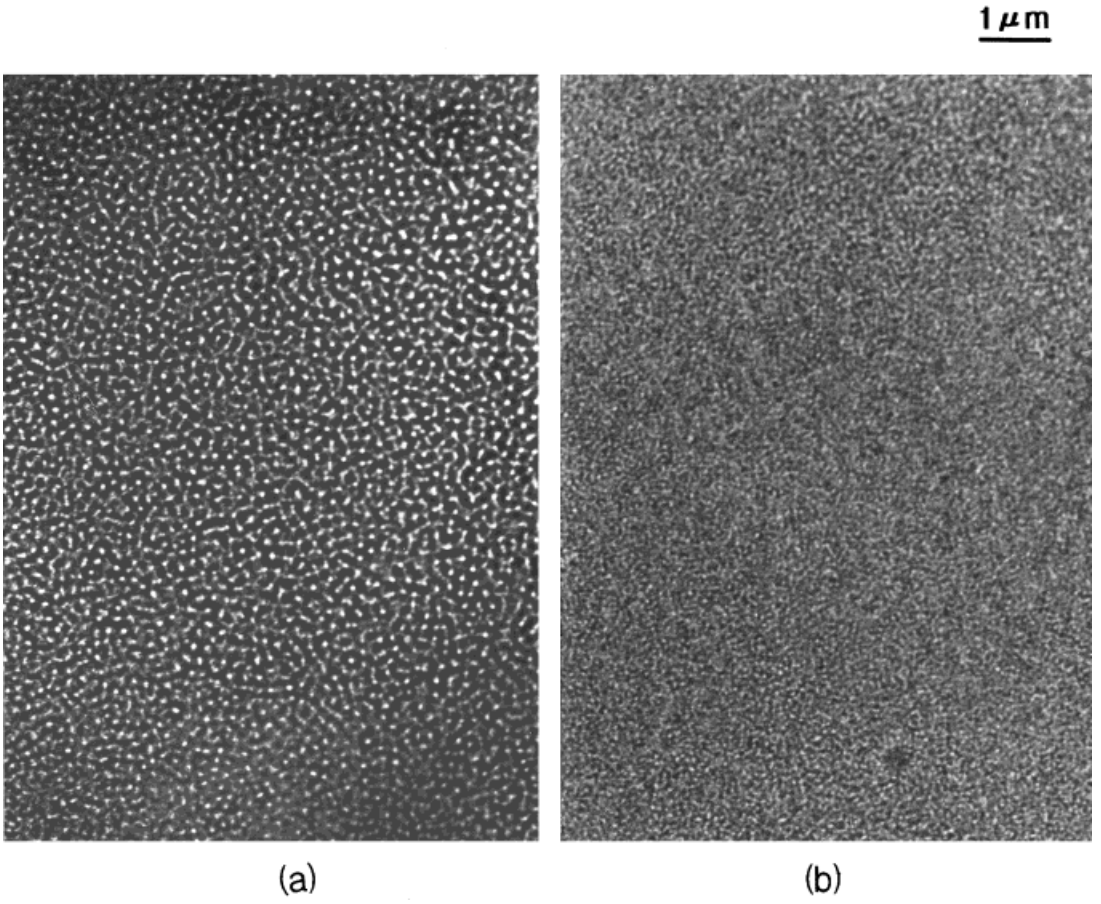

Figure 9 Optical micrographs of (a) (BPA + PNP)–Hexa–SAN-0 and (b) SAN-25 (1.6 + 14.4)/4/80 wt %) mixtures cured at 180°C.

nols in total phenols, the higher the SAN composition, and the lower the cure temperature, the shorter the Λ_m.

REFERENCES

1. N. J. L. Megson, *Phenolic Resin Chemistry,* Butterworth Press, London, 1958.
2. A. Knop and W. Scheib, *Chemistry and Application of Phenolic Resins,* Springer-Verlag, New York, 1979.
3. A. Tanaka and R. Nakatsuka, *J. Adhes. Soc. Jpn.,* **1,** 97 (1980).
4. C. B. Bucknall and I. K. Patridge, *Polymer,* **24,** 639 (1980).
5. R. S. Raghava, *J. Polym. Sci., Polym. Phys. Ed.,* **25,** 1017 (1987).
6. K. Yamanaka and T. Inoue, *Polymer,* **30,** 662 (1989).
7. B. S. Kim, T. Chiba, and T. Inoue, *Polymer,* **34,** 2809 (1993).
8. B. S. Kim, T. Chiba, and T. Inoue, *Polymer,* **36,** 43, 67 (1995).
9. B. S. Kim and T. Inoue, *Polymer,* **36,** 1985 (1995).
10. B. S. Kim, *J. Appl. Polym. Sci.,* **65,** 85 (1997).
11. *Br. Plast. Rubber,* July/Aug., 33 (1990).
12. S. Shu and S. Konii, *Jpn. Kokai Tokkyo Koho,* JP 73051046 (1973).
13. B. M. Culbertson, O. Tiba, and M. L. Deviney, in *Proceedings of the 34th International SAMPE Symposium,* 1989, p. 2483.
14. A. Matsumoto, K. Hasegawa, A. Fukuda, and K. Otsuki, *J. Appl. Polym. Sci.,* **44,** 205 (1992).
15. B. S. Kim, *Korea Polym. J.,* **5,** 84 (1997).
16. B. S. Kim, G. Nakamura, and T. Inoue, *J. Appl. Polym. Sci.,* **68,** 1829 (1998).
17. J. Koberstein, T. P. Russel, and R. S. Stein, *J. Polym. Sci., Polym. Phys. Ed.,* **17,** 1719 (1979).
18. P. J. Flory, *Principles of Polymer Chemistry,* Cornell University Press, Ithaca, New York, 1953.
19. W. H. Stockmayer, *J. Chem. Phys.,* **11,** 45 (1943).
20. C. W. Macosko and D. R. Miller, *Macromolecules,* **9,** 199 (1976).